Eur Biophys J (2003) 32: 47–54
DOI 10.1007/s00249-002-0264-9

ARTICLE

**Daniel Huster · Peter Müller · Klaus Arnold
Andreas Herrmann**

Dynamics of lipid chain attached fluorophore 7-nitrobenz-2-oxa-1,3-diazol-4-yl (NBD) in negatively charged membranes determined by NMR spectroscopy

Received: 27 July 2002 / Accepted: 3 October 2002 / Published online: 14 November 2002

Abstract We have determined the average location and dynamic reorientation of the fluorophore 7-nitrobenz-2-oxa-1,3-diazol-4-yl (NBD) attached to a C12 *sn*-2 chain of a phosphatidylserine (PS) analogue (C12-NBD-PS) in zwitterionic phosphatidylcholine (PC) and negatively charged phosphatidylserine (PS) host membranes. ^{1}H magic angle spinning nuclear Overhauser enhancement spectroscopy indicates a highly dynamic reorientation of the aromatic molecule in the membrane. The average location of NBD is characterized by a broad distribution function along the membrane director with a maximum indicating the location of the probe in the lipid/water interface of the lipid membrane. This behavior can be explained by a backfolding of the *sn*-2 chain towards the aqueous phase. Small differences in the distribution profiles of the NBD group along the membrane normal between PC and PS host membranes were found: in a PC host membrane, the NBD distribution has its maximum in the glycerol region; in a PS host membrane, NBD resides mostly in the upper chain region. These differences may be accounted for by packing differences in the PC versus PS host membranes. As seen by ^{2}H NMR order parameters, PS bilayers show a much higher packing density compared to PC membranes. Consequently, backfolding of the *sn*-2 chain with the NBD group attached causes a larger decrease of molecular order of the *sn*-1 chain in PS than in PC membranes. The broad distributions obtained for lipid chain attached NBD molecules reflect the motional freedom and molecular disorder in the liquid-crystalline lipid membrane.

Keywords Magic angle spinning NOESY · Deuterium NMR · Model membranes · Phospholipid analogues · Looping back

D. Huster (✉)
Junior Research Group "Solid-state NMR Studies of Membrane-associated Proteins",
Biotechnological-Biomedical Center,
University of Leipzig, Liebigstrasse 27,
04103 Leipzig, Germany
E-mail: husd@medizin.uni-leipzig.de
Tel.: +49-341-9715706
Fax: +49-341-9715709

P. Müller · A. Herrmann
Institute of Biology/Biophysics,
Humboldt-University Berlin,
Invalidenstrasse 43, 10115 Berlin, Germany

K. Arnold
Institute of Medical Physics and Biophysics,
University of Leipzig, Liebigstrasse 27,
04103 Leipzig, Germany

Introduction

To study intracellular lipid trafficking, labeled lipid analogues are often used. For instance, to follow the intracellular route and the transbilayer dynamics of phospholipids within various biological membranes, phospholipid analogues are employed that bear a palmitoyl or myristoyl chain in the *sn*-1 position and a fatty acid chain of varying length to which a fluorescent 7-nitrobenz-2-oxa-1,3-diazol-4-yl (NBD) group is linked in the *sn*-2 position (see Fig. 1) (Comfurius et al. 1990; Connor et al. 1990, 1994; Colleau et al. 1991; Smeets et al. 1994; Pomorski et al. 1996, 1999; Tang et al. 1996; Hrafnsdottir et al. 1997). Typically, the fatty acid chain in the *sn*-2 position is shorter (C6 or C12), allowing a rather rapid incorporation of analogues into lipid membranes (in particular in the case of C6). However, analogues with a longer fatty acid chain in the *sn*-2 position are more reliable reporters of respective endogenous phospholipids (Devaux et al. 2002).

Several studies have investigated the localization of the NBD group of phospholipid analogues parallel to the bilayer normal by (1) applying paramagnetic fluorescence quenching by spin labels or (2) exploiting fluorescence properties in media of varying dielectric properties (Chattopadhyay and London 1987; Mazeres et al. 1996). These investigations revealed that the charged aromatic NBD probe has a propensity for a

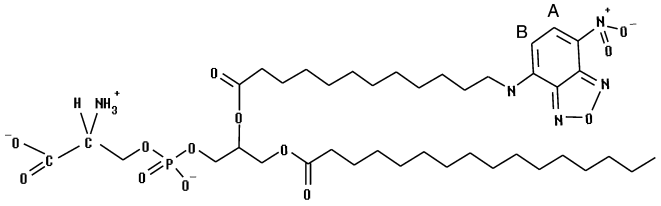

Fig. 1 Chemical structure of the phospholipid analogue C12-NBD-PS investigated in this study. The protons on the ring system utilized for the magnetization exchange with lipid signals measured in the NOESY experiment are labeled *A* and *B*

more polar environment, which causes a looping back of the entire *sn*-2 chain. This localizes the fluorescent moiety to the lipid/water interface of the membrane, which is stabilized by a complex force balance of electrostatic and nonpolar interactions (Huster et al. 2001). Since NBD is an aromatic molecule with fixed charges and a strong dipole moment, favorable electrostatic interactions provide the driving force for the preferential localization of the NBD group to the more polar environment of the lipid/water interface. Such a structural arrangement represents the lowest free energy configuration of the NBD ring system. However, the probe shows a very dynamic reorientation, resulting in a broad transversal distribution along the bilayer normal. Indeed, we found finite probabilities of localization also in the lower acyl chain as well as in the headgroup region (Huster et al. 2001). This highly dynamic reorientation of the NBD probe is a consequence of the general molecular disorder and dynamic structural variety of all molecular segments in phospholipid membranes revealed by recent X-ray studies (Wiener and White 1992; White and Wiener 1996; Petrache et al. 1998), ^{1}H magic angle spinning (MAS) NMR measurements (Huster et al. 1999; Feller et al. 1999) and molecular dynamics simulations (Pastor and Feller 1996; Feller et al. 1999). In accordance with this, small molecules partitioned into membranes such as ethanol or indole analogues exhibit a broad dynamic distribution in the membrane rather than a confined location (Holte and Gawrisch 1997). This reflects the dynamic roughness of the membrane surface and the variety of fast motions and structural heterogeneity of the lipid membrane (Persson et al. 1998; Yau et al. 1998).

In this study, we have characterized the location of the NBD group linked to a phosphatidylserine (PS) analogue (C12-NBD-PS, Fig. 1) in membranes of varying negative surface potential. This analogue has been employed, for example, to investigate transbilayer phospholipid asymmetry in biological membranes (for a review, see Devaux et al. 2002). Since PS is enriched on the cytoplasmic leaflet of eukaryotic membranes, giving rise to negative surface potential at intracellular pH, the influence of the surface charge on NBD localization is of particular relevance. We have used ^{1}H MAS nuclear Overhauser enhancement spectroscopy (^{1}H MAS NOESY) to determine the localization of the NBD group parallel to the bilayer normal. The ^{1}H MAS NOESY method allows us to measure cross-relaxation rates that represent contact probabilities between NBD and the protons in all lipid segments in a quantitative fashion (Huster and Gawrisch 1999; Huster et al. 1999). Thus, the transversal distribution profile of NBD can be determined.

Similar to the behavior of NBD analogues of PC in zwitterionic membranes (Huster et al. 2001), a preferential localization of the probe in the lipid/water interface region was found for the respective PS analogue. However, in contrast to the PC analogue, for C12-NBD-PS the distribution of NBD along the membrane normal was significantly broader and appeared to depend on the lipid packing density of the host matrix. This study shows that when using C12-NBD-PS as a probe for studying the structural organization and dynamics of membranes as, for example, derived from FRET studies or fluorescence quenching assays, the dynamic localization of the fluorescence moiety has to be considered.

Materials and methods

Materials

1-Palmitoyl-2-[12-[(7-nitro-2,1,3-benzoxadiazol-4-yl)amino]dodecanoyl]-*sn*-glycero-3-phosphoserine (C12-NBD-PS), 1-palmitoyl-2-[6-[(7-nitro-2,1,3-benzoxadiazol-4-yl)amino]dodecanoyl]-*sn*-glycero-3-phosphocholine (C6-NBD-PC), 1-palmitoyl-2-oleoyl-*sn*-glycero-3-phosphocholine (POPC), 1-palmitoyl-2-oleoyl-*sn*-glycero-3-phosphoserine (POPS), 1-stearoyl-d_{35}-2-oleoyl-*sn*-glycero-3-phosphocholine (SOPC-d_{35}) and 1-stearoyl-d_{35}-2-oleoyl-*sn*-glycero-3-phosphoserine (SOPS-d_{35}) were purchased from Avanti Polar Lipids (Alabaster, Ala., USA) and used without further purification. The chemical structure of the analogue C12-NBD-PS is depicted in Fig. 1.

For reducing the NO_2^- group of NBD to an NH_2 group, an aqueous suspension of 2.6 mM C6-NBD-PC was incubated with 167 mM dithionite for 10 min at 37 °C. At this concentration the phospholipid analogue forms micelles and the NBD group of all analogue molecules is readily accessible by dithionite. The reaction of the fluorophore with dithionite was accompanied by a color change from yellow/orange to dark red. Reduced C6-NBD-PC was extracted from the aqueous dithionite suspension by adding chloroform/methanol (2:1) The extraction was repeated once by evaporating the solvent of the chloroform phase, adding buffer and, subsequently, a second addition of chloroform/methanol (2:1). While dithionite remains in the aqueous phase, the NBD lipid analogue can be separated in the chloroform/methanol phase.

Sample preparation

Aliquots of phospholipids and NBD analogues were mixed in chloroform and evaporated under a stream of nitrogen. The lipid film was then redissolved in approximately 500 μL cyclohexane and lyophilized in a vacuum of ~80 μbar. The resulting lipid powder was hydrated to 50 wt% with buffer solution (10 mM Hepes, 1 mM or 300 mM NaCl, pH 7.4) prepared in D_2O for ^{1}H measurements and deuterium-depleted H_2O for ^{2}H experiments. The samples were freeze-thawed, vortexed, stirred, and gently centrifuged for equilibration of the lipid water suspension. Subsequently, lipid samples were transferred into 4-mm MAS rotors with spherical inserts for MAS NMR experiments and sealed. For ^{2}H NMR experiments, samples were transferred to 5-mm glass tubes and sealed.

^{1}H Magic-angle spinning NMR

^{1}H MAS NMR experiments were carried out on a Bruker DRX600 spectrometer (Bruker Analytische Messtechnik, Rheinstetten) operating at a resonance frequency of 600.13 MHz for ^{1}H at a temperature of 30 °C. The MAS spinning frequency was 10 kHz. Spectra were acquired at a spectrum width of 10 kHz with a typical 90°-pulse length of 6.6 μs. Two-dimensional NOESY experiments (Jeener et al. 1979; Wagner and Wüthrich 1982) were carried out with phase cycling in the States-TPPI mode at mixing times of 1, 150, 300, and 450 ms. A total of 380 complex data points were collected in the indirect dimensions with 16 transients per increment at a relaxation delay of 3.5 s between successive scans, yielding a total acquisition time of approximately 6 h per spectrum. A square sine-bell window function was used in both dimensions for processing.

Peak volumes in 2D NOESY spectra were integrated using the Bruker XWINNMR software package. NOE build-up curves were fitted to a spin pair model (Macura and Ernst 1980), yielding cross-relaxation rates (σ_{ij}) according to:

$$A_{ij}(t_m) = (A_{jj}(0)/2)(1 - \exp(-2\sigma_{ij}t_m))\exp(-t_m/T_{ij}) \quad (1)$$

where the variable $A_{ij}(t_m)$ represents the cross-peak volume at mixing time t_m and $A_{jj}(0)$ the diagonal peak volume at mixing time zero. The value $1/T_{ij}$ defines the rate of magnetization leakage towards the lattice. Cross-relaxation rates were obtained from fitting of experimental cross-peak volumes at varying mixing times to Eq. (1) using the nonlinear regression curve fitter in SigmaPlot (Jandel Scientific Software, San Rafael, Calif., USA).

^{2}H Solid-state NMR

^{2}H NMR spectra were recorded on a Bruker DRX300 NMR spectrometer operating at a resonance frequency of 46.07 MHz for ^{2}H using a double-channel solids probe equipped with a 5-mm solenoid coil. The ^{2}H spectra were accumulated at a spectrum width of 500 kHz using a phase-cycled quadrupolar echo sequence (Davis et al. 1976) and a relaxation delay of 500 ms. The two 5.4-μs $\pi/2$ pulses were separated by a 100 μs delay. Spectra were left shifted after acquisition to start Fourier transformation on top of the quadrupolar echo. A 100 Hz exponential line broadening was applied.

The ^{2}H NMR powder spectra were depaked (McCabe and Wassall 1995) and smoothed order parameter profiles (Lafleur et al. 1989) were determined from the observed quadrupolar splittings ($\Delta\nu_Q$) according to:

$$\Delta\nu_Q = \frac{3}{4}\frac{e^2qQ}{h}S(n) \quad (2)$$

where e^2qQ/h represents the quadrupolar coupling constant (167 kHz for ^{2}H in the C-^{2}H bond) and $S(n)$ the chain order parameter for the nth carbon position in the chain. Average order parameters were calculated by adding all order parameters and dividing them by the number of deuterated groups in the chain.

Results and discussion

In Fig. 1 the chemical structure of the C12-NBD-PS phospholipid analogue used in this study is shown. To determine the localization of the NBD group in the membrane, we first carried out ^{2}H order parameter measurements. In Fig. 2, typical spectra of SOPS-d_{35} in the absence and presence of 25 mol% C12-NBD-PS are shown. Depaking of these spectra yields order parameters for the entire *sn*-1 chain (not shown). For the localization of the NBD moiety in the membrane, difference order parameter profiles are meaningful since they indicate at which position the lipid chain order is perturbed due to the presence of NBD analogues. We have investigated three samples with varying negative surface potentials.

In Fig. 3 difference order parameters for C12-NBD-PS/SOPC and C12-NBD-PS/SOPS are shown, both at low ionic strength (1 mM NaCl, 10 mM Hepes, pH 7.4), as well as for C12-NBD-PS/SOPS at high ionic strength

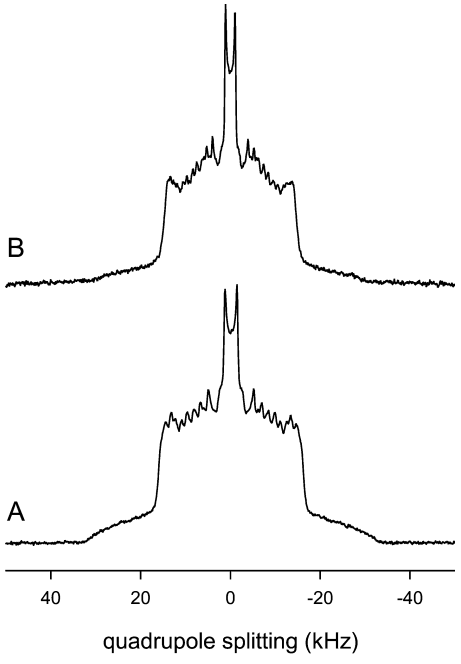

Fig. 2 ^{2}H NMR spectra of SOPS-d_{35} multilamellar membrane preparations in the absence (**A**) and presence (**B**) of 25 mol% C12-NBD-PS at a temperature of 30 °C. Samples contained 50 wt% buffer (1 mM NaCl, 10 mM Hepes, pH 7.4)

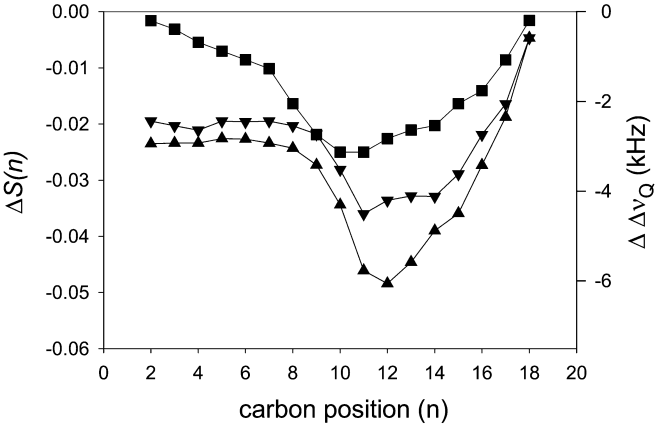

Fig. 3 Difference order parameter profiles of SOPC-d_{35}/C12-NBD-PS (*squares*) and SOPS-d_{35}/C12-NBD-PS (*down triangles*), both at 1 mM NaCl, 10 mM Hepes, pH 7.4, and SOPS-d_{35}/C12-NBD-PS (*up triangles*) at 300 mM NaCl, 10 mM Hepes, pH 7.4 at 30 °C. Difference order parameters are obtained by subtraction of order parameters in the absence of C12-NBD-PS from order parameters in the presence of C12-NBD-PS

(300 mM NaCl, 10 mM Hepes, pH 7.4), with regard to pure SOPC and SOPS membranes under identical conditions. For all three samples the presence of C12-NBD-PS leads to a reduction of chain order of the host matrix. For comparison, Table 1 shows the average order parameters for all samples investigated. However, the changes in molecular order do not occur homogeneously along the lipid chain. While the order decreases moderately in the upper chain region, a significant decrease is observed in the lower half of the chain. Such changes are in agreement with an interface location of the NBD group, as observed previously for the PC NBD analogues in POPC (Huster et al. 2001). Owing to the location of NBD in the interface region of the membrane, the lower chain segments experience a larger free volume and correspondingly lower chain order.

The smallest order decrease is seen for the PC membranes. It is interesting to note that PC membranes are more loosely packed than PS bilayers (Table 1), which agrees with previous results (Huster et al. 1998). Therefore, the interface location of the NBD moiety and the backfolding of the *sn*-2 chain causes a more drastic disordering for the PS membranes. There are significant variations in the difference order parameter profiles for PC and PS host membranes. For PC, order parameters decrease rather gradually from the C2 position to the middle part of the chain. However, only a very small order reduction is observed in the upper chain for PC membranes. For PS membranes, both at high and low ionic strength the order of the upper chain half is significantly reduced in the presence of C12-NBD-PS, almost independent of the position. Nevertheless, a drop in molecular order occurs for lower chain segments. This is more pronounced for PS membranes at a high ionic strength of 300 mM NaCl. These results may indicate differences in the average location of the NBD group, depending on the lipid composition of the bilayer.

Quantitative data about the localization of NBD are obtained from quantitative 2D MAS NOESY measurements. Figure 4 shows a ^{1}H MAS NMR spectrum of a mixture of C12-NBD-PS and POPC (molar ratio: 1:3) at a spinning speed of 10 kHz. Resonance assignment is shown in the figure according to the literature (Neumann et al. 1985; Forbes et al. 1988; Sparling et al. 1989; Volke and Pampel 1995). The assignment of the PS headgroup signals was confirmed by means of a MAS HMQC spectrum (not shown). As revealed by a double quantum filtered COSY experiment in chloroform solution under high-resolution NMR conditions, the methylene group in the *sn*-2 chain next to the nitrogen (see Fig. 1) is superimposed on the signal of the CH_2-N of the PC headgroup (β protons at 3.7 ppm). The other methylene signals of the short fatty acid chain appear slightly downfield shifted from most of the chain methylene signals at 1.5 ppm and 1.8 ppm. The proton signals of NBD were assigned according to the reference of pure NBD provided in the Integrated Spectral Data Base System for Organic Compounds (http://www.aist.go.jp/RIODB/SDBS/).

The NMR signal of proton B of the NBD ring system (see Fig. 1) is rather narrow while proton A exhibits some broadening. The same broadening of signal A was observed for the PC-NBD analogues (Huster et al. 2001). As we have suggested previously, the origin of this broadening could be related to the vicinity of the charged dipole on the ring system (Huster et al. 2001). If that holds true, the two NBD signals should be of identical linewidth if the NO_2 dipole is reduced to a NH_2 group. For comparison, the aromatic region of the ^{1}H MAS spectrum of reduced C6-NBD-PC is also shown in Fig. 4. Indeed, the two NBD signals show the same line width after reduction of the NBD dipole, suggesting that the fixed charges are responsible for the line broadening of signal A. The assignment of the NBD A and B signals of reduced NBD was confirmed by a ^{1}H MAS NOESY spectrum. The upfield shift of both signals indicates the change in the electronic environment of these protons. Some impurities that might

Table 1 Average order parameters of the perdeuterated stearic acid in SOPC-d_{35} and SOPS-d_{35} and their mixtures with C12-NBD-PS at varying ionic strengths at 30°C in buffer (10 mM Hepes, pH 7.4)

Membrane system	Ionic strength	S_{av}
SOPC-d_{35}	1 mM NaCl	0.156
SOPC-d_{35}/C12-NBD-PS (3:1)	1 mM NaCl	0.143
SOPS-d_{35}	1 mM NaCl	0.194
SOPS-d_{35}/C12-NBD-PS (3:1)	1 mM NaCl	0.170
SOPS-d_{35}	300 mM NaCl	0.200
SOPS-d_{35}/C12-NBD-PS (3:1)	300 mM NaCl	0.171

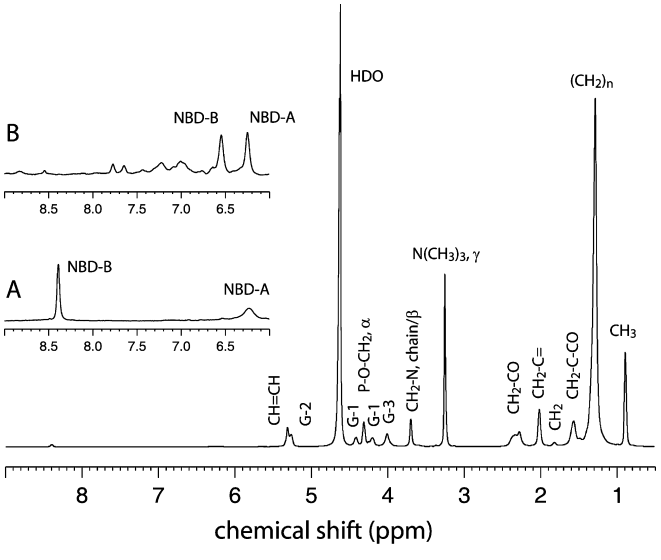

Fig. 4 600.1 MHz ^{1}H MAS spectrum of C12-NBD-PS in a POPC phospholipid matrix at 50 wt% D_2O buffer (1 mM NaCl, 10 mM Hepes, pH 7.4) at a spinning speed of 10 kHz and a temperature of 30 °C. *Inset*: **A** shows the downfield region of the spectrum with the proton signals from the NBD ring system at a 20-fold amplification. **B** shows the downfield region of the spectrum of reduced C6-NBD-PC in POPC. The molar ratio of NBD analogues and POPC was 1:3

be due to residual dithionite in the sample are also observed in that spectrum.

In order to characterize the location of the NBD group in the membrane, 2D NOESY spectra were recorded for mixtures of C12-NBD-PS in POPC or POPS. In Fig. 5 a contour plot of the NBD-B region of the 2D NOESY spectrum of C12-NBD-PS/POPS (1:3, mol/mol, 1 mM NaCl, 10 mM Hepes, pH 7.4) at a mixing time of 300 ms is plotted, showing the well-resolved cross-peaks of the B signal of the NBD ring with all other lipid signals. Recently, it was shown that lipid-lipid cross-peaks in multilamellar vesicles are of intermolecular origin, with the exception of directly neighboring methylene groups in the acyl chains (Huster et al. 1999). As is obvious from Fig. 5, there is also a strong intramolecular cross-peak between the two NBD protons due to their close proximity. The presence of cross-peaks of NBD protons with all lipid signals indicates that the NBD probe must be broadly distributed over the entire membrane normal, ranging from the headgroup to the lipid chain terminus. The observed intensity differences between the cross-peaks are due to

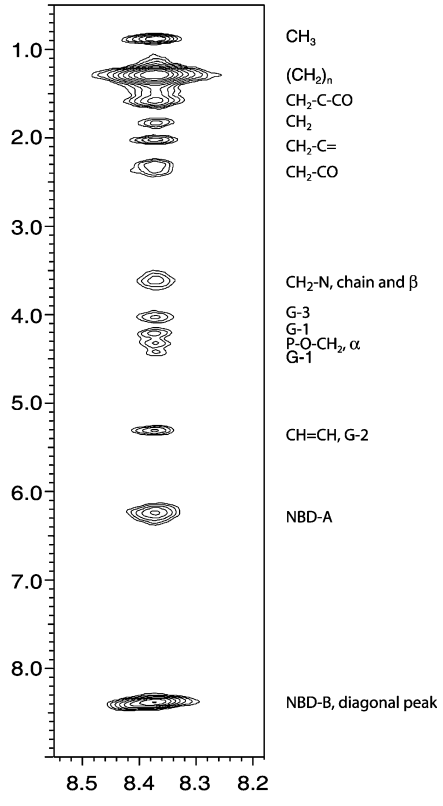

Fig. 5 Contour plot of the NBD-B region of a 600.1 MHz ^{1}H MAS NOESY spectrum of C12-NBD-PS in POPS membranes (1 mM NaCl, 10 mM Hepes, pH 7.4) at a spinning speed of 10 kHz and a temperature of 30 °C. The mixing time was 300 ms. The slice shows the cross-peaks of the NBD-B proton with all other lipid signals. Data were recorded in a phase-sensitive mode; all cross-peaks have positive intensity. A total of 16 transients per t_1 increment have been accumulated, yielding a total acquisition time of approximately 6 h. The molar ratio of NBD analogues and POPC was 1:3

varying numbers of protons contributing to the magnetization exchange, as well as to differences in the contact probability between those protons. Therefore, only a quantitative analysis of cross-relaxation rates provides insight into the location of the NBD group in the lipid bilayer.

To this end, the NOESY cross-peaks were integrated and cross-relaxation rates determined according to Eq. (1). The dependence of cross-peak volumes on mixing time can be well fitted with the spin pair exchange model (Macura and Ernst 1980). The reproducibility of cross-relaxation rate determination between independent experiments is typically around ±10–15% (Huster and Gawrisch 1999). Intermolecular cross-relaxation rates can be interpreted as contact probabilities between lipid segments if all magnetization transfer processes occur with the same correlation time. For lipid membranes, this provides a reasonable approximation since NOE transfers are modulated largely by slow motions of the entire lipid molecules, such as lateral diffusion (Feller et al. 1999; Yau and Gawrisch 2000). The large variety of faster motions with a multitude of correlation times does not contribute significant spectral density to the intermolecular cross-relaxation process (Feller et al. 1999; Yau and Gawrisch 2000). Further, the influence of spin diffusion on magnetization exchange can be neglected at the short mixing times used in this study (Huster and Gawrisch 1999).

Absolute cross-relaxation rates for the contacts between the NBD ring protons and various phospholipid protons were calculated and plotted as a function of the average position along the membrane normal (Fig. 6). The transversal distribution profile of the fluorescence probe in the membrane is presented for C12-NBD-PS/POPC and C12-NBD-PS/POPS at low ionic strength (1 mM NaCl, 10 mM Hepes, pH 7.4) (Fig. 6A and B, respectively) as well as for C12-NBD-PS/POPS at high ionic strength (300 mM NaCl, 10 mM Hepes, pH 7.4) (Fig. 6C). In all mixtures, the molar ratio between phospholipid and NBD analogue was 3:1. The cross-relaxation rates in zwitterionic membranes are about a factor 2 lower than in negatively charged membranes. This can be explained by small correlation time differences due to packing differences in PC and PS membranes.

The transversal distribution function of the NBD label attached to the *sn*-2 chain of C12-NBD-PS in membranes with a negative surface potential reveals an average location of the fluorescence probe in the lipid/water interface of the membrane for all three samples. A similar location of the NBD moiety was found for the respective NBD-PC analogue in zwitterionic membranes, which requires a backfolding of the *sn*-2 chain towards the aqueous phase (Chattopadhyay and London 1987). A comparable behavior was also established for C12-NBD-PS analogues in zwitterionic and negatively charged host membranes (Mazeres et al. 1996). However, these studies did not consider the dynamic reorientation and the distribution width of the NBD

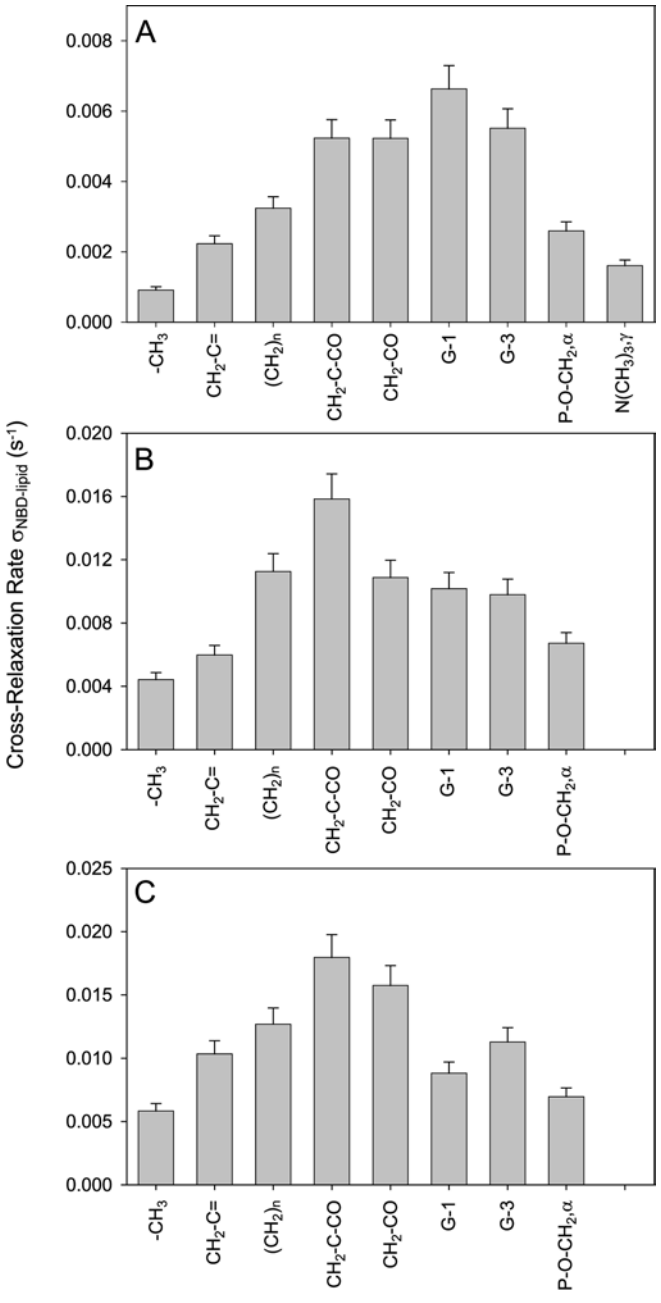

Fig. 6 Cross-relaxation rates (s^{-1}) between the B proton of the NBD ring system (see Fig. 1 for assignment) and protons of phospholipid analogues for **A** C12-NBD-PS/POPC (1 mM NaCl, 10 mM Hepes, pH 7.4), **B** C12-NBD-PS/POPS (1 mM NaCl, 10 mM Hepes, pH 7.4) and **C** C12-NBD-PS/POPS (300 mM NaCl, 10 mM Hepes, pH 7.4). The molar ratio between NBD analogue and phospholipid was 1:3. Cross-relaxation rates represent the contact probability for the B proton of the NBD group with the respective protons of POPC (Huster et al. 1999). Cross-relaxation rates were calculated using the two-spin exchange model (Macura and Ernst 1980) according to Eq. (1). The *error bars* represent a typical error estimate of 10%

probe in membranes. According to our data, the NBD fluorophore has a preferential location in the lipid water interface of the membrane (glycerol/upper chain region) but may also extend into the headgroup as well as the lower, hydrophobic chain region. Such broad distributions of lipid-attached probe molecules are in agreement with more recent models of the liquid crystalline lipid bilayer conveyed by latest X-ray (White and Wiener 1996; Petrache et al. 1998) and NMR (Huster et al. 1999) investigations, as well as molecular dynamics simulations (Venable et al. 1993). According to these studies, the location of lipid segments parallel to the bilayer normal varies by many angstroms due to thermal motions, resulting in a high degree of structural heterogeneity. Consequently, lipid-attached probe molecules experience a similar molecular disorder.

In a previous study we have characterized the transversal distribution function of NBD of PC analogues (C6-NBD-PC and C12-NBD-PC) in POPC membranes (Huster et al. 2001). While we also found a broad distribution along the bilayer normal in zwitterionic membranes, the distribution of the NBD probe showed a more pronounced maximum in the interface region and lower cross-relaxation rates with lower chain segments or the headgroup. Apparently the negative surface charge of the vesicles influences the average position of the NBD moiety within the membrane, leading to a broader distribution with a higher probability of localization in the middle and lower chain region compared to uncharged bilayers.

In our earlier paper we discussed the factors that might contribute to the lowest free energy location of the *sn*-2 chain-attached NBD probe in the membrane (Huster et al. 2001). On the one hand, aromatic compounds such as NBD have a high propensity for the nonpolar environment of the membrane due to the hydrophobic effect, which provides a driving force for the probe towards the membrane interior. On the other hand, NBD is a charged molecule that possesses both fixed charges and a dipole moment, which gives rise to strong electrostatic interactions with the fixed charges of the lipid headgroup and the CO and water dipole moments in the lipid/water interface (Gawrisch et al. 1992). Further, favorable hydrogen bonding and cation-π interactions (Dougherty 1996) and lipid-induced contributions such as lipid matrix properties and the lipid packing density have to be considered in the discussion of the NBD location with the lowest free energy.

In this study we have employed membranes of different surface potential to investigate the influence of electrostatic interactions on the location and dynamic distribution of the NBD probe C12-NBD-PS. As mentioned above, the distribution of the NBD moiety in negatively charged membranes is broader than in zwitterionic bilayers, with a higher probability of NBD location in the lower chain region of the membrane. Furthermore, in C12-NBD-PS/POPC the NBD group shows a preferential location in the glycerol region, while the NBD distribution is biased towards the upper chain region for C12-NBD-PS/POPS membranes. While variation of the surface potential may provide an explanation for these differences, we note that the changes do not follow a simple correlation with the strength of

the negative surface potentials Ψ_0. For the C12-NBD-PS/POPC sample (1 mM NaCl) a surface potential of $\Psi_0 = -182$ mV is calculated from the modified Graham equation that includes binding of monovalent Na^+ ions to the membrane surface (Ohki et al. 1982). For C12-NBD-PS/POPS membranes, surface potentials of $\Psi_0 = -253$ mV and $\Psi_0 = -105$ mV are calculated in the presence of 1 mM and 300 mM NaCl, respectively. Since the surface potential of the C12-NBD-PS/POPC membranes falls right between the values obtained for the C12-NBD-PS/POPS samples at varying ionic strength, the differences in the NBD location cannot be explained solely according to differences in the surface potentials.

Unfortunately, to assess the influence of the other physical interactions in the lipid/water interface that might contribute to the NBD location of lowest free energy is not straightforward. Both PC and PS headgroups possess fixed charges for favorable electrostatic interactions with the NBD group in the complex electrostatic environment of the bilayer surface. Moreover, both headgroups provide hydrogen bond acceptors as well as a positive charge for attractive cation-π interactions.

In order to characterize a contribution of the charged dipole on the NBD ring system, we have tried to determine the average location of reduced NBD in C6-NBD-PC in the lipid membrane. As a result of a chemical reaction with dithionite, which abolishes the fixed charges of the ring system, the charged NO_2^- group of NBD is converted into an uncharged NH_2 (McIntyre and Sleight 1991). Unfortunately, the stability of reduced C6-NBD-PC was not sufficient to allow a determination of the average location of the probe by ^{1}H MAS NOESY experiments, which requires sample stability over more than 24 h.

One may wonder if lipid chain packing properties have an impact on the location of the NBD group. It has already been shown that these properties influence the location of small molecules in the lipid/water interface (Holte and Gawrisch 1997). Indeed, there is a strong difference in the packing properties of SOPC and SOPS membranes (Table 1). The lipid chain order parameter is about 25% higher in SOPS than in SOPC membranes. In other words, SOPS membranes have a much higher packing density than SOPC bilayers. These differences may explain the different average distribution profiles of the NBD group linked to C12-NBD-PS in SOPC and SOPS host membranes. The NBD moiety is a rather bulky group of a molecular volume of approximately 160 Å^3. An interface location of the group requires a significant decrease in lipid packing density, as seen in Fig. 3. This process requires more energy in the more densely packed SOPS matrix than in a less densely packed SOPC bilayer. Consequently, a backfolding of the NBD-*sn*-2 chain causes a much larger reduction of lipid chain order in SOPS membranes than in SOPC membranes (Fig. 3). We speculate that a slightly deeper location of the NBD moiety in the upper chain of SOPS host membranes is energetically more favorable than a location in the glycerol region observed in SOPC host membranes. Therefore, in the SOPS host matrix the average location of NBD shows its maximum in the upper chain region rather than in the glycerol as in the case of a SOPC host matrix.

Finally, we note that the ^{1}H NMR measurements of this study were carried out in POPC/POPS while the ^{2}H NMR was conducted in SOPC/SOPS. However, this small variation is unlikely to measurably influence the NBD location and dynamic reorientation of the probe in the membranes.

Conclusions

Backfolding of the lipid-attached NBD probe to the lipid/water interface is observed in negatively charged as well as in zwitterionic membranes. As opposed to neutral bilayers, the distribution profiles of the NBD moiety are broader in negatively charged membranes. The distribution width almost equals the width of one entire membrane leaflet. Apart from the surface potential, lipid packing of the host membranes also affects the average location of the fluorescence group. This observation may be important for the location of the probe in bilayers containing cholesterol as biological membranes, which will be a topic of an upcoming study.

Acknowledgements The work was supported by the Deutsche Forschungsgemeinschaft (Ar 195/8-1 to K.A., He1928 to A.H. and Mu1017 to P.M.) and the Saxon State Ministry of Higher Education, Research and Culture (Junior Research Group "Solid-state NMR Studies of Membrane-associated Proteins"). The authors would like to thank Dr. Klaus Gawrisch for the SOPC-d_{35} and the SOPS-d_{35}. We are grateful to Mrs. S. Schiller for her technical assistance.

References

Chattopadhyay A, London E (1987) Parallax method for direct measurement of membrane penetration depth utilizing fluorescence quenching by spin-labeled phospholipids. Biochemistry 26:39–45

Colleau M, Herve P, Fellmann P, Devaux PF (1991) Transmembrane diffusion of fluorescent phospholipids in human erythrocytes. Chem Phys Lipids 57:29–37

Comfurius P, Senden JM, Tilly RH, Schroit AJ, Bevers EM, Zwaal RF (1990) Loss of membrane phospholipid asymmetry in platelets and red cells may be associated with calcium-induced shedding of plasma membrane and inhibition of aminophospholipid translocase. Biochim Biophys Acta 1026:153–160

Connor J, Gillum K, Schroit AJ (1990) Maintenance of lipid asymmetry in red blood cells and ghosts: effect of divalent cations and serum albumin on the transbilayer distribution of phosphatidylserine. Biochim Biophys Acta 1025:82–86

Connor J, Pak CC, Schroit AJ (1994) Exposure of phosphatidylserine in the outer leaflet of human red blood cells. Relationship to cell density, cell age, and clearance by mononuclear cells. J Biol Chem 269:2399–2404

Davis JH, Jeffrey KR, Bloom M, Valic MI, Higgs TP (1976) Quadrupolar echo deuteron magnetic resonance spectroscopy in ordered hydrocarbon chains. Chem Phys Lett 42:390–394

Devaux PF, Fellmann P, Herve P (2002) Investigation on lipid asymmetry using lipid probes. Comparison between spin-labeled lipids and fluorescent lipids. Chem Phys Lipids 116:115–134

Dougherty DA (1996) Cation-pi interactions in chemistry and biology: a new view of benzene, Phe, Tyr, and Trp. Science 271:163–168

Feller SE, Huster D, Gawrisch K (1999) Interpretation of NOESY cross-relaxation rates from molecular dynamics simulations of a lipid bilayer. J Am Chem Soc 121:8963–8964

Forbes J, Husted C, Oldfield E (1988) High-field, high-resolution proton "magic-angle" sample-spinning nuclear magnetic resonance spectroscopic studies of gel and liquid crystalline lipid bilayers and the effects of cholesterol. J Am Chem Soc 110:1059–1065

Gawrisch K, Ruston D, Zimmerberg J, Parsegian VA, Rand RP, Fuller N (1992) Membrane dipole potentials, hydration forces, and the ordering of water at membrane surfaces. Biophys J 61:1213–1223

Holte LL, Gawrisch K (1997) Determining ethanol distribution in phospholipid multilayers with MAS-NOESY spectra. Biochemistry 36:4669–4674

Hrafnsdottir S, Nichols JW, Menon AK (1997) Transbilayer movement of fluorescent phospholipids in *Bacillus megaterium* membrane vesicles. Biochemistry 36:4969–4978

Huster D, Gawrisch K (1999) NOESY NMR crosspeaks between lipid headgroups and hydrocarbon chains: spin diffusion or molecular disorder? J Am Chem Soc 121:1992–1993

Huster D, Arnold K, Gawrisch K (1998) Influence of docosahexaenoic acid and cholesterol on lateral lipid organization in phospholipid membranes. Biochemistry 37:17299–17308

Huster D, Arnold K, Gawrisch K (1999) Investigation of lipid organization in biological membranes by two-dimensional nuclear Overhauser enhancement spectroscopy. J Phys Chem B 103:243–251

Huster D, Müller P, Arnold K, Herrmann A (2001) Dynamics of membrane penetration of the fluorescent 7-nitrobenz-2-oxa-1,3-diazol-4-yl (NBD) group attached to an acyl chain of phosphatidylcholine. Biophys J 80:822–831

Jeener J, Meier BH, Bachmann P, Ernst RR (1979) Investigation of exchange processes by two-dimensional NMR spectroscopy. J Chem Phys 71:4546–4553

Lafleur M, Fine B, Sternin E, Cullis PR, Bloom M (1989) Smoothed orientational order profile of lipid bilayers by ^{2}H-nuclear magnetic resonance. Biophys J 56:1037–1041

Macura S, Ernst RR (1980) Elucidation of cross relaxation in liquids by two-dimensional N.M.R. spectroscopy. Mol Phys 41:95–117

Mazeres S, Schram V, Tocanne JF, Lopez A (1996) 7-Nitrobenz-2-oxa-1,3-diazole-4-yl-labeled phospholipids in lipid membranes: differences in fluorescence behavior. Biophys J 71:327–335

McCabe MA, Wassall SR (1995) Fast-Fourier-transform depaking. J Magn Reson B 106:80–82

McIntyre JC, Sleight RG (1991) Fluorescence assay for phospholipid membrane asymmetry. Biochemistry 30:11819–11827

Neumann J-M, Zachowski A, Trandinh S, Devaux PF (1985) High-resolution proton magnetic-resonance of sonicated phospholipids. Eur Biophys J 11:219–223

Ohki S, Düzgünes N, Leonards K (1982) Phospholipid vesicle aggregation: effect of monovalent and divalent ions. Biochemistry 21:2127–2133

Pastor RW, Feller SE (1996) Time scales of lipid dynamics and molecular dynamics. In: Merz KM, Roux B (eds) Biological membanes. A molecular perspective from computation and experiment. Birkhäuser, Boston, pp 3–30

Persson S, Killian JA, Lindblom G (1998) Molecular ordering of interfacially localized tryptophan analogs in ester- and ether-lipid bilayers studied by ^{2}H-NMR. Biophys J 75:1365–1371

Petrache HI, Gouliaev N, Tristram-Nagle S, Zhang R, Suter RM, Nagle JF (1998) Interbilayer interactions from high resolution x-ray scattering. Phys Rev E 57:7014–7024

Pomorski T, Muller P, Zimmermann B, Burger K, Devaux PF, Herrmann A (1996) Transbilayer movement of fluorescent and spin-labeled phospholipids in the plasma membrane of human fibroblasts: a quantitative approach. J Cell Sci 109:687–698

Pomorski T, Herrmann A, Muller P, van Meer G, Burger K (1999) Protein-mediated inward translocation of phospholipids occurs in both the apical and basolateral plasma membrane domains of epithelial cells. Biochemistry 38:142–150

Smeets EF, Comfurius P, Bevers EM, Zwaal RF (1994) Calcium-induced transbilayer scrambling of fluorescent phospholipid analogs in platelets and erythrocytes. Biochim Biophys Acta 1195:281–286

Sparling ML, Zidovetzki R, Muller L, Chan SI (1989) Analysis of membrane lipids by 500 MHz ^{1}H NMR. Anal Biochem 178:67–76

Tang XJ, Halleck MS, Schlegel RA, Williamson P (1996) A subfamily of P-type ATPases with aminophospholipid transporting activity. Science 272:1495–1497

Venable RM, Zhang Y, Hardy BJ, Pastor RW (1993) Molecular dynamics simulations of a lipid bilayer and of hexadecane: an investigation of membrane fluidity. Science 262:223–226

Volke F, Pampel A (1995) Membrane hydration and structure on a subnanometer scale as seen by high resolution solid state nuclear magnetic resonance: POPC and POPC/$C_{12}EO_4$ model membranes. Biophys J 68:1960–1965

Wagner G, Wüthrich K (1982) Sequential resonance assignments in protein ^{1}H nuclear magnetic resonance spectra. J Mol Biol 155:347–366

White SH, Wiener MC. (1996) The liquid-crystallographic structure of fluid lipid bilayer membranes. In: Merz KM, Roux B (eds) Biological membranes. A molecular perspective from computation and experiment. Birkhäuser, Boston, pp 127–144

Wiener MC, White SH (1992) Structure of a fluid dioleoylphosphatidylcholine bilayer determined by joint refinement of x-ray and neutron diffraction data. III. Complete structure. Biophys J 61:434–447

Yau WM, Gawrisch K (2000) Lateral lipid diffusion dominates NOESY cross-relaxation in membranes. J Am Chem Soc 122:3971–3972

Yau WM, Wimley WC, Gawrisch K, White SH (1998) The preference of tryptophan for membrane interfaces. Biochemistry 37:14713–14718